$4f$-$5d$ hybridization and the α-γ phase transition in cerium

Atsushi Fujimori* and J. H. Weaver
Department of Chemical Engineering and Materials Science, University of Minnesota, Minneapolis, Minnesota 55455
(Received 26 December 1984)

The α-γ phase transition in Ce metal is explained by $4f$-$5d$ hybridization effects. The α phase is identified with a state consisting of hybridized $4f^0$ and $4f^1$ configurations where, although the $4f^1$ component is dominant, the local magnetic moment is quenched via strong $4f$-$5d$ hybridization of the order of ~ 1 eV. Increased $4f$-$5d$ hybridization with decreasing volume stabilizes the α phase relative to the γ phase for small volumes. The pressure-volume and pressure-temperature diagrams have been calculated with use of this model, and the phase diagram of Ce has been well reproduced. The core-level photoemission, valence-band photoemission, and bremsstrahlung isochromat spectra of α- and γ-Ce have been calculated based on the same model, and good agreement with experiment has been obtained.

I. INTRODUCTION

There has been much controversy concerning the mechanism of the α-γ phase transition in Ce metal.[1,2] On going from the γ to α phase under pressure or on cooling, the lattice volume collapses by $\sim 15\%$ without changes in the crystal structure, and the local magnetic moment of the $Ce^{3+}(4f^1)$ ion disappears. The earlier $Ce^{3+} \rightarrow Ce^{4+}$ promotional models[3] have now been excluded on the basis of recent photoemission[4,5] and Compton scattering[6] experiments, band-structure calculations,[7] and theoretical thermodynamical arguments.[8] These have shown that the number of $4f$ electrons changes only slightly across the transition. Recently the $4f$-derived contributions to the valence-band photoemission have been reported to show double-peak structures.[4,5,9] These results have stimulated theoretical interests with relation to anomalous properties of Ce and its compounds.[10–14] The spectra suggest that interaction between $4f$ and valence electrons is important and that the $4f$ electrons are more hybridized in the α phase.[5] Core-level x-ray photoemission (XPS) and bremsstrahlung isochromat spectroscopy (BIS) have shown that the $4f$—valence-band hybridization is much greater (0.5—1 eV) than the traditionally accepted values (<0.1 eV) and increases in going from γ- to α-Ce.[15] Successful models for the α-γ transition must then be consistent with these recent results. On the other hand, it has been argued that the traditional small hybridization seems more appropriate to describe the low-energy properties such as magnetic susceptibilities, specific heats, and electrical resistivities.[16]

In the present paper, we present a simple model for the α-γ phase transition which is consistent with the above spectroscopic results. The α phase is identified with a state having strong $4f$-$5d$ hydbridization, where the loss of the $4f^1$ local magnetic moment and the volume collapse result from participation of $4f$ orbitals in bond formation with neighboring (and, to a lesser extent, distant-neighbor) $5d$ orbitals.[17] The bonding energy increases with decreasing volume because of the increasing $4f$-$5d$ orbital overlap and stabilizes the α phase, whereas the γ phase is stabilized by the intra-atomic correlation energy of the rare-earth ion (only spin-orbit energy in the case of Ce^{3+}) in the large-volume region. The $4f$-$5d$ hybridization strength necessary to reproduce the phase diagram will also be shown to explain the valence-band photoemission, core-level photoemission, and BIS spectra. We have given qualitative discussions of the α-γ transition based on a cluster model in a previous paper,[18] and the present paper gives its quantitative explanation and various electron spectra of α- and γ-Ce by using a more general but still simple model. Although we have not attempted calculations on the low-energy properties, the present model is proposed to show effectively small $4f$—conduction-band hybridization in the low-excitation-energy region and to be consistent with the observed low-energy behaviors as well as those of mixed-valence Ce compounds.

II. α-γ PHASE TRANSITION

First, we discuss the stability of the local $4f^1$ moment (γ-Ce) against $4f$-$5d$ hybridization by considering $4f$ photoemission process within a model where a single $4f$ ion interacts with $5d$—conduction-band electrons. If the $4f$ electron is emitted by photoemission, the remaining system relaxes to screen the $4f$ hole in various ways: The $4f^0$ hole may be either screened by $5d$ electrons on the hole site or screened by $4f$ electrons themselves. The latter process occurs via a $5d$—conduction-band$\rightarrow 4f$-level charge transfer, and the resulting $4f^1 5d^{-1}$ configuration, where $5d^{-1}$ denotes a hole in the $5d$ conduction band, would be with the highest probability a totally symmetric (singlet) state having no local magnetic moment, since the singlet $4f^1 5d^{-1}$ state would have the largest overlap with the (singlet) $4f^0$-hole state because of the same local symmetry, thus the large $4f$-$5d$ transfer integrals and the highest $5d \rightarrow 4f$ (monopole) transition probability. The $5d$—conduction-band hole in the $4f^1 5d^{-1}$ configuration does not have amplitude at the $4f$ site, as the $4f$ and $5d$ atomic orbitals on the same site have different symmetry. Therefore hybridization between the $4f$- and $5d$-band

states occurs via neighboring $4f$-$5d$ atomic-orbital components. Here we note that only the *occupied* part of the $5d$ band contributes to the $5d \rightarrow 4f$ charge transfer and that the $4f$-$5d$ hybridization strength is not constant within the occupied conduction band but is strongly energy dependent.[19] Thus the $5d$ hole is created mostly within an energy range of the width of 1 eV (around an energy position ϵ_{5d}) in spite of the large (~ 10 eV) total width of the Ce $5d$ band. A full relaxation, namely relaxation to the local-moment ground state $4f^1$ with $J=\frac{5}{2}$, may have a small transition probability as compared to the singlet $4f^1 5d^{-1}$ state. This argument implies that the lower-binding-energy component of the double $4f$ peaks does not have to be exactly located at (within thermal energies of) the Fermi level E_F but generally below it in magnetic Ce systems such as γ-Ce, and in fact this peak has been observed 0.2 eV below E_F by the high-resolution photoemission study of γ-Ce.[9] The two $4f$-derived peaks are thus attributed to two final-state configurations, $4f^0$ and $4f^1 5d^{-1}$, which are hybridized with each other.[20] If the $4f$-$5d$ hybridization increases, the lower-binding-energy $4f$ peak would become closer to E_F due to repulsion of the two hybridized final states and would finally be above E_F. Then the local-moment ground state becomes unstable, and a new phase having the nonmagnetic $4f^0$-$4f^1 5d^{-1}$ hybridized ground state is stabilized. The $4f^0$-$4f^1 5d^{-1}$ hybridized state is expected to be predominantly $4f^1$-like, because the $4f^0$ configuration is 1–2 eV above the $4f^1$ configuration.[8,21] We identify this phase as α-Ce.

The $4f$-$5d$ hybridization increases rapidly as the lattice volume decreases. Consequently the hybridized nonmagnetic state is stabilized relative to the local-moment state for smaller volumes as shown in Fig. 1, and the first-order α-γ transition takes place as a function of pressure. At high temperatures the γ phase is further stabilized by the $J=\frac{5}{2}$ entropy term ($TS=-k_B T \ln 6$) (where k_B is the Boltzmann constant), but for even higher temperatures the potential barrier between the two phases is overcome by thermal excitations and the phase boundary terminates at a critical point, giving rise to a pressure-temperature phase diagram as shown in Fig. 2(b).

The volume (v) dependence of the energy of the $4f^1$ configuration is assumed to have the form

$$E_1 = A[(v_0/v)^{2\lambda} - 2(v_0/v)^{\lambda}] , \quad (1)$$

where we set $A=4.25$ eV and $\lambda=0.8435$ in order to reproduce the cohesive energy of γ-Ce (Ref. 22) and the average bulk modulus of La and Pr (Ref. 23). As for the $4f^0$ configuration energy,

$$E_0 = E_1 + 1.2 + 2.0(1.12 v^{1/3} - 3.3)^2 , \quad (2)$$

where v is the Å^3 and energies are in eV, according to $4f^1 \rightarrow 4f^0$ excitation energies given by a renormalized-atom calculation.[21] The local-moment state is stabilized relative to Eq. (1) by the spin-orbit interaction ($2\xi_{4f}=0.14$ eV):

$$E_\gamma = E_1 - 2\xi_{4f} , \quad (3)$$

while the largely $4f^1$-like nonmagnetic state is stabilized

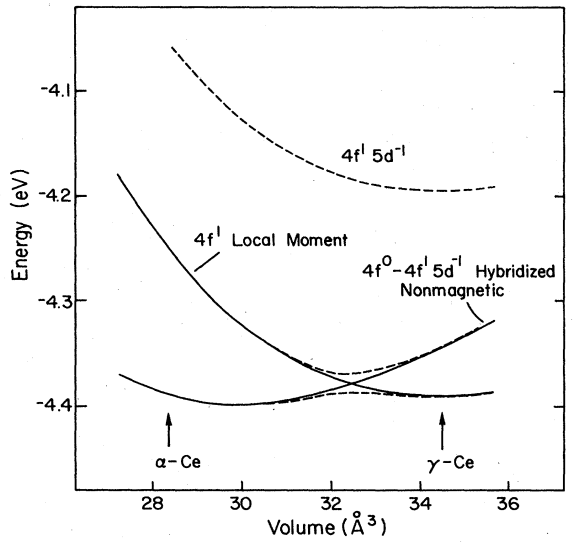

FIG. 1. Energies of the local-moment $4f^1$ state and the $4f^0$-$4f^1 5d^{-1}$ hybridized nonmagnetic state for Ce ($v_0=34.5$ Å, $V_0=0.48$ eV, $\epsilon_{5d}=-0.056$ eV) as a function of lattice volume. Energies of the unhybridized $4f^1 5d^{-1}$ configuration are shown by a dashed line. The free Ce atom is taken as the energy zero. The lattice volumes of γ-Ce ($P=0$, $T=300$ K) and α-Ce ($P=7.2$ kbar, $T=300$ K) are indicated. Weak hybridization between $4f$ and conduction electrons close to E_F would further perturb the energy diagram as shown by the dashed lines.

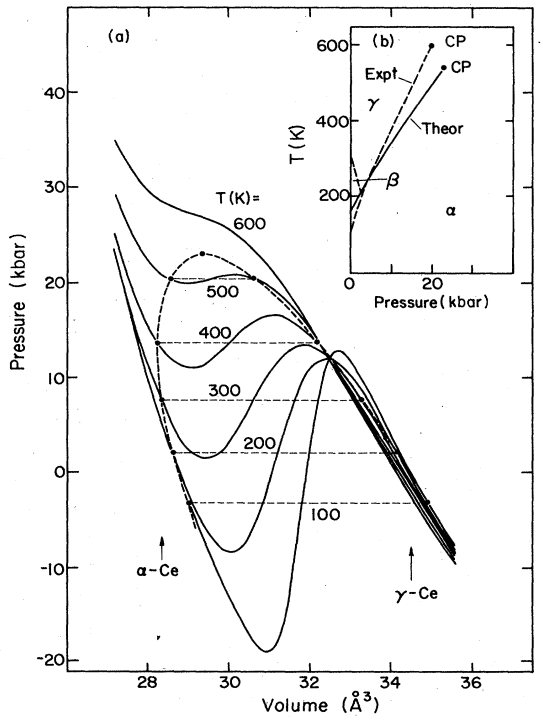

FIG. 2. (a) Pressure-volume diagrams as a function of temperature calculated using the parameter values given in text or in the caption of Fig. 1. First-order transitions are indicated by dashed lines. (b) Pressure-volume phase diagram of Ce obtained in the present work compared with experiments (Ref. 2).

relative to Eq. (1) through mixing with the $4f^0$ configuration:

$$E_\alpha=\{E_0+E_1-\epsilon_{5d}-[(E_0-E_1+\epsilon_{5d})^2+4V^2]^{1/2}\}/2\ , \tag{4}$$

where $-\epsilon_{5d}$ is a $5d$-hole energy relative to E_1 (not E_γ) and V is the effective matrix element between the $4f^0$ and $4f^15d^{-1}$ configurations. V is an appropriate sum[10,14] of transfer integrals between one-electron atomic $4f$ and bandlike $5d$ orbitals. As contributions from overlap between neighboring $4f$ and $5d$ atomic orbitals are the most important for V, we assume V to vary as a function of volume v as

$$V=V_0(v_0/v)^2\ , \tag{5}$$

utilizing a relation for muffing-tin orbitals.[24] The singlet $4f^15d^{-1}$ state is assumed to have the form

$$|4f^15d^{-1}\rangle^\nu=\sum_{i,j}a_{ij}^\nu f_i^\dagger d_j\,|4f^0\rangle\ , \tag{6}$$

analogous to the variational form of the mixed-valence ground state,[10,18,25] where the coefficients a_{ij}^ν give the proper symmetry.

Pressure-volume and pressure-temperature diagrams shown in Fig. 2 were calculated by adjusting parameters as $v_0=34.5$ Å^3, $V_0=0.48$ eV, and $\epsilon_{5d}=-0.056$ eV. We thus obtained a pressure induced volume collapse of 15% at $P=7.6$ kbar for $T=300$ K, a temperature-dependent one at $T\sim160$ K for $P=0$, and the first-order transition terminates at a critical point $P=23.2$ kbar and $T=540.0$ K, in reasonable agreement with experiment[2] (15% volume collapse at $P=8$ kbar for room temperature, at $T\sim150$ K for $P=0$, and a critical point at $P=20$ kbar and $T=600$ K). Furthermore, the calculated results show that a lattice stiffening occurs in going from the γ to α phase as has been observed experimentally.[26] It is also noted that the enthalpy difference between the α and γ phases (~1 kcal/mole) (Ref. 27) was correctly predicted.

III. PHOTOEMISSION AND BIS SPECTRA

Based on the present model, gross features (i.e., positions and intensities of principal spectral features, all multiple effects being neglected) in core-level photoemission, $4f$-derived photoemission, and BIS spectra have been calculated. Here again we have considered the narrow (~1 eV) occupied part of the $5d$ band, because the unoccupied part does not contribute significantly to any observed spectra (only a weak BIS peak close to E_F in γ-Ce may be due to the $4f^2\rightarrow4f^15d^1$ final-state transition). As the $4f^2$ configuration appears in the final states of core-level photoemission and BIS, the model is extended to include the $4f^2$ configuration. Then the ground state of γ-Ce is a mixture of the $4f^1$ and $4f^25d^{-1}$ configurations:

$$\Psi_\gamma=b_1\,|4f^1\rangle+b_2\,|4f^25d^{-1}\rangle\ , \tag{7}$$

although the mixing of the $4f^2$ configuration in the ground state is small because of the large Coulomb energy between two $4f$ electrons on the same site ($U\sim5$ eV) as compared to the $4f$-$5d$ hybridization ($V<1$ eV). The ground state can be obtained by solving a secular equation for the Hamiltonian:

$$\begin{bmatrix}0 & V\\ V & \epsilon_{4f}-\epsilon_{5d}+U\end{bmatrix}\ . \tag{8}$$

This ground state is further lowered by $2\xi_{4f}$ due to spin-orbit interaction. Note that the energy of the $4f^1$ configuration (without the spin-orbit interaction) as a function of lattice volume is given by Eq. (1) but is taken to be the energy zero in Eq. (8) and in the following calculations, so that $-\epsilon_{4f}=E_0-E_1$. As for the α-Ce ground state,

$$\Psi_\alpha=c_0\,|4f^0\rangle+c_1\,|4f^15d^{-1}\rangle+c_2\,|4f^24d^{-2}\rangle \tag{9}$$

and the Hamiltonian is

$$\begin{bmatrix}-\epsilon_{4f} & V & 0\\ V & -\epsilon_{5d} & V\\ 0 & V & \epsilon_{4f}-2\epsilon_{5d}+U\end{bmatrix}\ . \tag{10}$$

Final states for $4f$ photoemission in γ-Ce are given by the same form as that for the α-Ce ground state [Eq. (9)]:

$$\Psi_F=e_{F0}\,|4f^0\rangle+e_{F1}\,|4f^15d^{-1}\rangle \tag{11}$$

and the same Hamiltonian (10), since final states giving intense $4f$-derived lines are expected to be singlet. As for α-Ce, final states of $4f$ photoemission,

$$\Psi_F=f_{F0}\,|4f^05d^{-1}\rangle+g_{F1}\,|4f^15d^{-2}\rangle\ , \tag{12}$$

are obtained from

$$\begin{bmatrix}-\epsilon_{4f}-\epsilon_{5d} & V & 0\\ V & -2\epsilon_{5d} & V\\ 0 & V & \epsilon_{4f}-3\epsilon_{5d}+U\end{bmatrix}\ . \tag{13}$$

The $4f$ photoemission intensities are given as

$$I_F=|\,b_1a_{F0}\,|^2\ , \tag{14}$$

$$I_F=|\,c_1g_{F0}+c_2g_{F1}\,|^2\ , \tag{15}$$

for γ- and α-Ce, respectively.

The energy of the BIS final state of γ-Ce is simply given by $\epsilon_{4f}+U$ in the present approximation which neglects $4f\rightarrow5d$ charge transfer resulting in antiscreening, which may be responsible for a weak BIS feature just above E_F observed in γ-Ce.[28,14] Then BIS final states for α-Ce,

$$\Psi_F=h_{F1}\,|4f^1\rangle+h_{F2}\,|4f^25d^{-1}\rangle\ , \tag{16}$$

are described by the same Hamiltonian as that for the γ-Ce ground state, Eq. (8). The BIS intensities are given by

$$I_F=|\,b_1\,|^2\ , \tag{17}$$

$$I_F=|\,c_0h_{F1}+c_1h_{F2}\,|^2\ , \tag{18}$$

for γ- and α-Ce, respectively.

In calculating the $3d$ core-level photoemission spectra, another parameter, U_c, which represents the attractive Coulomb energy between the $3d$ core hole and the $4f$ electron, is introduced. Then the Hamiltonian for core-hole

final states in γ-Ce,

$$\Psi_F = k_{F1}\,|\,4f^1\rangle' + k_{F2}\,|\,4f^2 5d^{-1}\rangle' , \tag{19}$$

where the primes represent the $3d$ core hole, is given by

$$\begin{bmatrix} 0 & V \\ V & \epsilon_{4f} - \epsilon_{5d} + U - U_c \end{bmatrix} , \tag{20}$$

and the intensities by

$$I_F = |\,b_1 k_F + b_2 k_{F2}\,|^2 . \tag{21}$$

As for core-hole final states of α-Ce,

$$\Psi_F = P_{F0}\,|\,4f^0\rangle' + p_{F1}\,|\,4f^1 5d^{-1}\rangle' + p_{F2}\,|\,4f^2 5d^{-2}\rangle' , \tag{22}$$

the Hamiltonian is

$$\begin{bmatrix} U_c - \epsilon_{4f} & V & 0 \\ V & -\epsilon_{5d} & V \\ 0 & V & \epsilon_{4f} - 2\epsilon_{5d} + U - U_c \end{bmatrix} , \tag{23}$$

and the intensities

$$I_F = |\,c_0 p_{F0} + c_1 p_{F1} + c_2 p_{F2}\,|^2 . \tag{24}$$

In Eqs. (20) and (23), the energy zero is taken to be the $3d^9 4f^1$ core-hole state. V's are generally different for different spectroscopies and may differ by at most a few 10%. This is because of the fact that one of the $4f$ orbitals is occupied in the $4f^1 5d^{-1}$ configuration and thus the $4f^1 5d^{-1} \rightarrow 4f^2 5d^{-2}$ charge transfer is less effective than the $4f^0 \rightarrow 4f^1 5d^{-1}$ charge transfer.[14,19] However, we have assumed the same V in order to obtain a global fit to various spectroscopic results rather than to attempt the best fit for each spectrum.

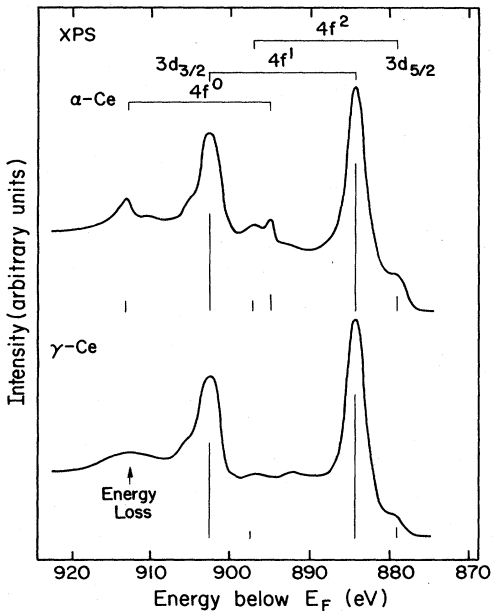

FIG. 3. Calculated $3d$ core-level XPS spectra for α- and γ-Ce (vertical bars) compared with experiment (Ref. 15). The energy zero in Eqs. (20) and (21) is set to be 883.8 and 901.9 eV for the $3d_{5/2}$ and $3d_{3/2}$ spin-orbit components, respectively.

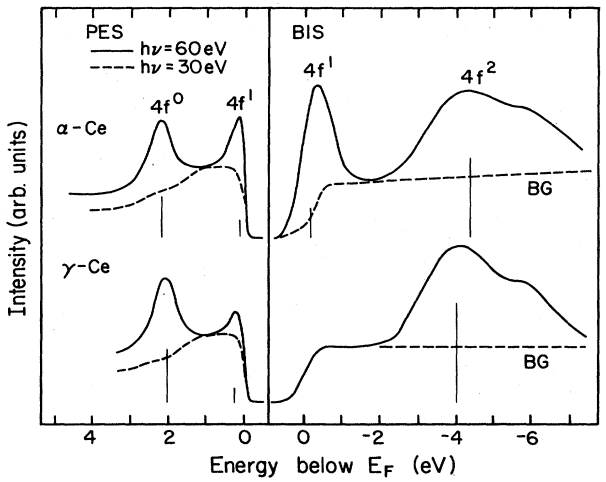

FIG. 4. Calculated $4f$-derived photoemission and BIS spectra for α- and γ-Ce compared with experiment (Refs. 9 and 15). Estimated non-$4f$-related emission ($\hbar\nu = 30$ eV) (Ref. 5) and backgrounds for BIS are also indicated. Multiplet structures in the BIS spectra have been neglected in the calculation.

Calculated spectra are shown in Figs. 3 and 4 and are compared with experiment.[5,9,15] Values for the parameters are listed in Table I, where corresponding parameters used to calculate the pressure-volume diagrams are also listed. For V and ϵ_{4f}, agreement with those obtained in the fit to the phase diagram is satisfactory considering that the spectroscopic and phase-diagram data were fitted independently and that the $4f^2$ configuration is included only in the spectral fit. On the other hand, ϵ_{5d} is systematically lower for the spectroscopies than for the phase diagram. This discrepancy is attributed to different meanings of ϵ_{5d} in the two cases: In the spectroscopies ϵ_{5d} represents the peak position in the $4f$-$5d$ hybridization strength, while in the thermal-quilibrium case it represents the highest ϵ_{5d} level hybridizing strongly with $4f$ in order to give the lowest $4f^1 5d^{-1}$ energy. Common values for U and U_c for α- and γ-Ce have been used (Table I) since these quantities are of single-atomic nature and would not differ much between α- and γ-Ce.

One can conclude from Figs. 3 and 4 that the calculated spectra reproduce the experimental ones quite well. In go-

TABLE I. Parameters used to calculate the photoemission and BIS spectra of α- and γ-Ce (in eV). Corresponding parameters used in the calculation of the pressure-volume and pressure-temperature diagrams (at $P = 7.6$ kbar and $T = 300$ K) are given in parentheses.

	ϵ_{4f}	ϵ_{5d}	V	U	U_c
γ-Ce	−1.55	−0.30	0.55	5.30	9.15
	(−1.44)	(−0.06)	(0.48)		
α-Ce	−1.50	−0.10	0.70	5.30	9.15
	(−1.23)	(−0.06)	(0.71)		

ing from γ- to α-Ce, $4f^0$ final-state features in the $3d$ core levels appear at the higher-binding-energy side of the $4f^1$ and $4f^2$ peaks due the $4f^0$ initial-state component in the α-Ce ground state (Fig. 3). Increased $4f^2$ satellite intensity in α-Ce is obviously due to increased hybridization V. As for the BIS spectra (Fig. 4), a peak appearing just above E_F for α-Ce is due to the $4f^0 \rightarrow 4f^1$ transition originating from the $4f^0$ initial-state component, and thus is not present in γ-Ce. A slight increase in the energy of the $4f^2$ BIS peak from γ-Ce to α-Ce is a consequence of energy lowering of the ground state due to hybridization in α-Ce. Among the Ce compounds it seems that the energy of the $4f^2$ BIS peak is systematically higher in nonmagnetic Ce compounds than in magnetic ones.[29]

The relative intensity change of the $4f$-derived double peaks across the $\gamma \rightarrow \alpha$ phase transition in the valence-band photoemission spectra (Fig. 4) results not only from increased hybridization but also from different symmetry characters of the ground states in the two phases. The $4f$ peak close to E_F in γ-Ce arises solely from final-state effects, namely the $4f^0 \rightarrow 4f^1 5d^{-1}$ final-state transition following the direct $4f^1 \rightarrow 4f^0$ photoemission, whereas in the α phase initial- and final-state effects cannot be clearly separated. Hence, the low-binding-energy $4f$ peak has a $4f^0$ final-state component due to the final-state $4f^0 5d^{-1}$-$4f^1 5d^{-2}$ mixing which is similar to the initial-state $4f^0$-$4f^1 5d^{-1}$ mixing and can result from a direct $4f^1 \rightarrow 4f^0$ photoemission process. The $4f$-derived photoemission of α-Ce is well described by the model of Gunnarsson and Schönhammer (GS),[10] where they assumed a nonmagnetic ground state of the type of Eq. (4), and the shallower $4f$ peak has been predicted at E_F in agreement with experiment.[9] On the other hand, in the γ phase, as discussed in Sec. II, the shallower $4f$ peak is not necessarily located very close to E_F, and the $4f$ intensity at E_F, which can be referred to as a Kondo peak and is responsible for low-energy phenomena, may be too weak to be observed by photoemission. In fact, the recent high-resolution photoemission study of γ-Ce (Ref. 9) has shown a $4f$ peak 0.2 eV below E_F (Ref. 30). In this respect we refer to a calculation of $4f$-derived photoemission spectra in trivalent Ce pnictides by Sakai *et al.*,[31] which gives an intense $4f$ peak well below E_F and a weak real Kondo peak at E_F.

The $4f$ occupancy was obtained to be 0.90 and 1.03 for α- and γ-Ce, respectively, which is consistent with Compton scattering[6] and band-structure calculations[7] which showed little $4f$ occupancy difference between the two phases.

IV. DISCUSSION

Valence-fluctuation phenomena have been considered to arise from two nearly degenerate $4f$ ionic configurations which interact weakly with conduction electrons near E_F, namely near degeneracy of the $4f^n(5d6s)^m$ and $4f^{n+1}(5d6s)^{m-1}$ configurations where $5d6s$ denotes conduction electrons. This picture has been confirmed by photoemission studies for Sm, Tm, and Eu compounds.[32] On the other hand, it has been found to be inappropriate for Ce systems because of the large $4f$—valence-band hybridization of the order of 1 eV, and electron-spectroscopic results had to be interpreted using models assuming large $4f$—valence-band hybridization (e.g., impurity Anderson model,[10] Ce-ligand cluster model[14,18]). However, the low-energy properties (e.g., static magnetic susceptibilities at finite temperatures,[1,2,33] infrared absorption[34]) have been interpreted based on the small $4f$—valence-band hybridization, and it has been inferred that the hybridization strength may differ in high-energy and low-energy experiments.[16,31,35]

In a previous paper,[36] we have proposed that for CeN valence fluctuation is occurring between the strongly hybridized nonmagnetic $4f^0$-$4f^1 L^{-1}$ state, where L^{-1} represents a ligand (N $2p$) hole, and the local-moment $4f^1$ state through weak $4f$-$5d$ hybridization, reconciling the strong $4f$—valence-band hybridization observed spectroscopically and the weak hybridization reflected on low-energy properties. That is, the $4f^0$-$4f^1 L^{-1}$ state plays an effective role of the $Ce^{4+}(4f^0)$ configuration as in the traditional valence-fluctuation picture. The present nonmagnetic $4f^0$-$4f^1 5d^{-1}$ state corresponds to the $4f^0 5d^{-1}$-$4f^1 L^{-1}$ state in CeN. The low-energy properties of mixed-valence Ce systems may result from the closeness of such a nonmagnetic state and the local-moment state. In Secs. II and III the two states have been viewed as well-defined eigenstates of the system, but they may further mix via weaker $4f$—conduction-band hybridization which has not been considered in the present model as illustrated in Fig. 1 by dashed lines.[37] The distinction between the strong and weak hybridization as done here would be appropriate only if the hybridization for states near E_F is weak as compared to states several tenths of eV below E_F, or deeper, and cannot be assumed *a priori* for all Ce systems. The $4f$—valence-band hybridization as a function of the valence-level energy based on realistic electronic structure as has been done for Ce pnictides[31] would be necessary to see the appropriateness of the distinction between strong and weak hybridization. On the other hand, it has recently been shown that a characteristic temperature proportional to the Kondo temperature scales anomalous magnetic, thermal, and electrical properties of mixed-valence compounds as well as trivalent compounds.[38] Therefore the particular form of the $4f$—valence-band hybridization term such as the peak at ϵ_{5d} assumed for Ce metal might not generally be necessary for existence of the two different energy scales in mixed-valence Ce compounds. Possibly the weak hybridization would correspond to residual hybridization after having projected out the strong hybridization by arbitrarily assuming the local-moment state (without any $4f$—valence-band interaction) and the nonmagnetic state [consisting of the $4f^1 5d^{-1}$ configuration of the form of Eq. (6) and the $4f^0$ configuration].

In the case of Ce metal, the local moment of the γ phase has been suggested not far from an instability while it seems to be well quenched in the α phase from the local magnetic susceptibility measured by the perturbed angular-correlation method.[39] Further, the valence of γ-Ce has been determined to be slightly larger than 3 by various methods.[1,2] This fact may be understood in terms of Fig. 1, where the local-moment state in the γ phase is not stable enough with respect to thermal energies or the

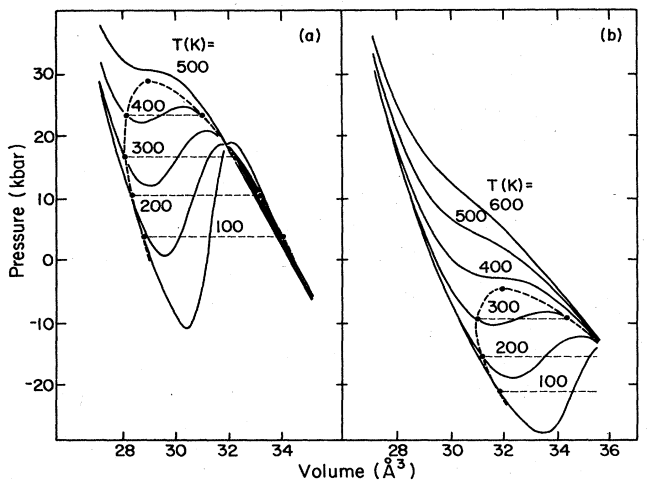

FIG. 5. (a) Pressure-volume diagrams as a function of temperature calculated using $V_0=0.46$ eV and $\epsilon_{5d}=-0.056$ eV corresponding to a Ce compound with a stable valence at atmospheric pressure but which undergoes a volume collapse at high pressures, and (b) those calculated using $V_0=0.46$ eV and $\epsilon_{5d}=0.03$ eV, which correspond to a mixed-valence Ce compound showing anomalous thermal expansion.

weak $4f$—conduction-band hybridization, while the nonmagnetic state in α-Ce is quite stable with respect to them.

The double minimum character of the ground-state energy as a function of volume (Fig. 1) which gives rise to the α-γ transition under moderate temperatures and pressures has resulted from a rather detailed balance of intraatomic (i.e., $4f^1 \rightarrow 4f^0$ excitation energies, spin-orbit interaction) and interatomic (i.e., $4f$—valence-band hybridization, extra-atomic relaxation) interactions. The relative stability of the magnetic and nonmagnetic states is greatly affected by small changes in the relevant parameters (V_0, ϵ_{5d}, ϵ_{4f}), and therefore the phase diagram is sensitively dependent on them. In order to see effects of varying parameters, we calculated pressure-volume diagrams for using a smaller V_0 and obtained a volume collapse at higher pressures for a trivalent Ce compound [Fig. 5(a)]. By using a higher value for ϵ_{5d}, the system was calculated to be α-like at ambient conditions and to show anomalous thermal expansion as has been observed for various mixed-valence compounds [Fig. 5(b)].[1,40]

Finally we would like to comment on the relation between the present model and another successful model, the Kondo—volume-collapse model,[41] according to which rapid increase of the Kondo temperature with decreasing volume leads to a large Kondo-singlet energy ($\sim$0.1 eV) in the volume-collapsed α phase. This would correspond to our case where the $4f$ electron and $5d$ hole form a singlet state due to the increased $4f$-$5d$ hybridization in the α phase. However, the low-temperature properties are different for the two models probably because of neglecting low-energy excitations in the vicinity of E_F in the present approach: In the Kondo model the α-γ transition terminates at another critical point at low temperature and negative pressure, which has been observed in an alloy system $La_xCe_{0.9-x}Th_{0.1}$.[42] This two-critical-point behavior comes from a general property of Fermi liquids which has not been incorporated in the present model.

V. CONCLUSION

We have assumed that the hybridization between atomiclike $4f$ states and $5d$-band states is a driving force for the α-γ phase transition in Ce metal. Based on this assumption, pressure-volume and pressure-temperature diagrams have been calculated to be in good agreement with experiment. Satellite structures in the core-level and $4f$-level photoemission spectra and the BIS spectra of α- and γ-Ce have also been calculated using parameters which are consistent with the phase diagram. The α phase is identified with a state derived from strong hybridization between $4f^0$ and $4f^15d^{-1}$ configurations, and therefore has no local magnetic moment despite the $4f$ occupancy close to 1. The assumed $4f$-$5d$ hybridization is $V\sim0.5$ eV for γ-Ce and $V\sim0.7$ eV for α-Ce, consistent with the $4f$-band width due to $4f$-$5d$ hybridization in the local-density energy bands of Ce.[7] While the large $4f$-$5d$ hybridization considered in the present work determines the gross features of the electron spectra and the α-γ transition energetics, we have to invoke weaker $4f$-$5d$ hybridization, which couples with low-energy excitations in the vicinity of E_F in order to explain the slightly unstable $4f^1$ local moment of γ-Ce and the line shapes of the spectra.

ACKNOWLEDGMENT

This work was supported by the National Science Foundation under Grant No. DMR-82-16489 (Solid State Chemistry Program).

*Permanent and present address: National Institute for Research in Inorganic Materials, Sakura-mura, Niihari-gun, Ibaraki 305, Japan.

[1]See, for example, J. M. Lawrence, P. S. Riseborough, and R. D. Parks, Rep. Prog. Phys. **41**, 1 (1981).

[2]D. C. Koskenmaki and K. A. Gschneidner, Jr., in *Handbook of the Physics and Chemistry of the Rare Earths,* edited by K. A. Gschneidner, Jr. and L. Eyring (North-Holland, Amsterdam, 1978), Vol. 1, p. 337.

[3]P. B. Coqblin and A. Blandin, Adv. Phys. **17**, 281 (1968); R. Ramirez and L. M. Falicov, Phys. Rev. B **3**, (1971); L. L. Hirst, J. Phys. Chem. Solids **35**, 1285 (1974).

[4]N. Mårtensson, B. Reihl, and R. D. Parks, Solid State Commun. **41**, 573 (1982).

[5]D. Wieliczka, J. H. Weaver, D. W. Lynch, and C. G. Olson, Phys. Rev. B **26**, 7056 (1982).

[6]U. Kornstädt, R. Lässer, and B. Lengeler, Phys. Rev. B **21**, 1898 (1980).

[7]D. Glötzel, J. Phys. F **8**, L163 (1978); W. E. Pickett, A. J. Freeman, and D. D. Koelling, Phys. Rev. B **23**, 1266 (1981).

[8]B. Johansson, Philos. Mag. **30**, 469 (1974); J. Phys. Chem. Solids **39**, 467 (1978).

[9]D. Wieliczka, C. G. Olson, and D. W. Lynch, Phys. Rev. B **29**, 3028 (1984).

[10]O. Gunnarsson and K. Schönhammer, Phys. Rev. Lett. **50**, 604 (1983); Phys. Rev. B **28**, 4315 (1983).

[11]S. H. Liu and K.-M. Ho, Phys. Rev. B **26**, 7052 (1982); **28**, 4220 (1983).

[12]M. R. Norman, D. D. Koelling, A. J. Freeman, H. J. F. Jansen, B. I. Min, T. Oguchi, and L. Ye, Phys. Rev. Lett. **53**, 1673 (1984).

[13]P. Riseborogh, J. Magn. Magn. Mater. (to be published).

[14]A. Fujimori, Phys. Rev. B **27**, 3992 (1983).

[15]E. Wuilloud, H. R. Moser, W.-D. Schneider, and Y. Baer, Phys. Rev. B **28**, 7354 (1983). Note the different definitions for the hybridization parameter between that used here and in Refs. 14 and 19 (V), and that in this reference and Ref. 10 (Δ).

[16]H. Kojima, Y. Kuramoto, and M. Tachiki, Z. Phys. B **54**, 293 (1984).

[17]A. Fujimori, M. Grioni, J. Joyce, and J. H. Weaver, Phys. Rev. B **31**, 8291 (1985).

[18]A. Fujimori, Phys. Rev. B **28**, 4489 (1983).

[19]The energy dependence of the $4f$-$5d$ hybridization strength is supported by photoemission spectra for Pr [D. Wieliczka, C. G. Olson, and D. W. Lynch, Phys. Rev. Lett. **52**, 2180 (1984)], where the shallower $4f$ peak is observed 0.5—1 eV below E_F, as constant $4f$—valence-band hybridization would yield the $4f$ peak at E_F. Further support comes from molecular-orbital calculations on small transition-metal clusters [R. P. Messmer, S. K. Knudson, K. H. Johnson, J. B. Diamond, and C. Y. Yang, Phys. Rev. B **13**, 1396 (1976)], where molecular orbitals that are allowed to mix with $4f$ by symmetry are not uniformly distributed in the occupied valence band but are grouped in the range 0.1—1 eV below E_F.

[20]In the $4f^0$ configuration, $5d$ electrons screen the $4f^0$-hole site via a $5d$-band→screening-$5d$-orbital transition, but are not explicitly indicated in the following notation. The $4f^0$ hole should thus be considered to be renormalized by the $5d$ screening (Ref. 12).

[21]J. Herbst and J. W. Wilkins, Phys. Rev. B **29**, 5992 (1984); J. F. Herbst, R. E. Watson, and J. W. Wilkins, *ibid.* **13**, 1439 (1976).

[22]K. A. Gschneidner, Jr., in *Solid State Physics,* edited by H. Ehrenreich, F. Seitz, and D. Turnbull (Academic, New York, 1964), Vol. 16, p. 275.

[23]T. E. Scott, in *Handbook of the Physics and Chemistry of the Rare Earths,* Ref. 2, p. 701.

[24]W. A. Harrison, *Electronic Structure and the Properties of Solids* (Freeman, San Francisco, 1980).

[25]C. M. Varma and Y. Yafet, Phys. Rev. B **13**, 2950 (1976).

[26]F. F. Voronov, V. A. Goncharova, and O. V. Stal'gorova, Zh. Eksp. Teor. Fiz. **76**, 1351 (1979) [Sov. Phys.—JETP **49**, 687 (1979)].

[27]R. I. Beecroft and C. A. Swenson, J. Phys. Chem. Solids **15**, 234 (1960).

[28]Y. Baer, H. R. Ott, J. C. Fuggle, L. E. DeLong, Phys. Rev. B **24**, 5384 (1981).

[29]An alternative explanation for the 0.2-eV peak is relaxation of the $4f^0$ state into the $J=\frac{7}{2}$ state of $4f^1$. The intensity of the $J=\frac{7}{2}$ peak has been calculated to be small in Ref. 31 but to be large in Ref. 38, depending on the assumption of the band structure.

[30]F. U. Hillebrecht, J. C. Fuggle, G. A. Sawatzky, M. Campagna, O. Gunnarsson, and K. Schönhammer, Phys. Rev. B **27**, 4637 (1983).

[31]O. Sakai, H. Takahashi, M. Takeshige, and T. Kasuya, Solid State Commun. **52**, 997 (1984).

[32]M. Campagna, G. K. Wertheim, and Y. Baer, in *Photoemission in Solids,* edited by L. Ley and M. Cardona (Springer, Berlin, 1979), Vol. 2, p. 217.

[33]A. Bringer and H. Lustfeld, Z. Phys. B **28**, 213 (1977).

[34]F. E. Pinkerton, B. C. Webb, A. J. Sievers, and J. W. Wilkins, Phys. Rev. B **30**, 3068 (1984).

[35]In Kondo systems the low-energy properties are compatible with strong $4f$—conduction-band hybridization [J. W. Allen, S.-J. Oh, I. Lindau, J. M. Lawrence, L. I. Johansson, and S. B. Hagström, Phys. Rev. Lett. **45**, 1100 (1981); M. Croft, J. H. Weaver, D. J. Peterman, and A. Franciosi, *ibid.* **46**, 1104 (1981)]. The dynamical susceptibility was also shown to be a function of ϵ_{4f}/Δ [O. Gunnarsson (unpublished)].

[36]A. Fujimori and J. H. Weaver, Phys. Rev. B **31**, 6345 (1985).

[37]The calculated pressure-temperature diagram would not be sensitive to the weak hybridization, because it would only make dull the pressure-volume diagrams at low temperatures.

[38]N. E. Brickers, D. L. Cox, and J. W. Wilkins, Phys. Rev. Lett. **54**, 320 (1984).

[39]H. H. Berchat, C. Broude, E. Dafni, F. D. Davidovski, M. Haas, and P. M. S. Lesser, Solid State Commun. **47**, 525 (1983); H. H. Berchat, H.-E. Hanke, E. Dafni, F. D. Davidovski, and M. Hass, Phys. Lett. **101A**, 507 (1984).

[40]R. Takke, M. Niksch, W. Assmus, B. Lüthi, R. Pott, R. Schefzky, and D. K. Wohlleben, Z. Phys. B **44**, 33 (1981).

[41]J. W. Allen and R. M. Martin, Phys. Rev. Lett. **49**, 1106 (1982); M. Lavagna, C. Lacroix, and M. Cyrot, J. Phys. F **13**, 1007 (1983).

[42]J. D. Thompson, Z. Fisk, J. M. Lawrence, J. L. Smith, and R. M. Martin, Phys. Rev. Lett. **50**, 1081 (1983); J. M. Lawrence, J. D. Thompson, Z. Fisk, J. L. Smith, and B. Batlogg, Phys. Rev. B **29**, 4017 (1984).